Thermogravimetric Analysis−Fourier Transform Infrared Analysis of Palm Oil Waste Pyrolysis

ARTICLE *in* ENERGY & FUELS · OCTOBER 2004

Impact Factor: 2.79 · DOI: 10.1021/ef030193m

6 AUTHORS, INCLUDING:

Yang Haiping
Huazhong University of Science and Technol…

64 PUBLICATIONS **2,343** CITATIONS

SEE PROFILE

Thermogravimetric Analysis−Fourier Transform Infrared Analysis of Palm Oil Waste Pyrolysis

Haiping Yang,[†,‡] Rong Yan,[*,†] Terence Chin,[†] David Tee Liang,[†] Hanping Chen,[‡] and Chuguang Zheng[‡]

Institute of Environmental Science and Engineering, Nanyang Technological University, Innovation Center, Block 2, Unit 237, 18 Nanyang Drive, Singapore 637723, and National Laboratory of Coal Combustion, Huazhong University of Science and Technology, Wuhan, 430074, People's Republic of China

Received December 22, 2003. Revised Manuscript Received August 4, 2004

The purpose of this study is to determine the pyrolysis characteristics and gas product properties of palm oil wastes, to promote a general idea of converting the wastes to an energy source. The palm oil waste contains ∼50 wt % carbon, 7 wt % hydrogen, and a trace amount of ash. The low heat value (LHV) of these wastes is ∼20 MJ/kg. They are ideal energy sources for biofuel generation. Thermal analysis demonstrates that these wastes are easily decomposed, with most of their weight lost from 220 °C to 340 °C at slow heating rates. The pyrolysis process could be divided into four stages: moisture evaporation, hemicellulose decomposition, cellulose decomposition, and lignin degradation. The kinetic analysis showed that the reaction order for the pyrolysis of palm oil wastes and three model biomass components (hemicellulose, cellulose, and lignin) is 1. The activation energy of the palm oil wastes is ∼60 kJ/mol. The decomposition process is prolonged and the maximum mass loss rate is decreased when the heating rate is increased from 0.1 °C/min to 100 °C/min. Varying the particle size from 250 μm to >2 mm has no significant influence on pyrolysis. The main gaseous products from the pyrolysis of palm oil waste are identified using thermogravimetric analysis−Fourier transform infrared (TGA−FTIR) spectroscopy, and, particularly, their real-time evolution characteristics are investigated. This fundamental study provides a basic insight of the palm oil waste pyrolysis, which can benefit our current work in developing an advanced thermal processes for high-yield biofuel production from palm oil waste.

1. Introduction

Almost 80% of the world's palm oil is produced in southeast Asia. With the sharp expansion of palm oil demand and production, palm oil wastes (empty fruit bunches (EFB), fiber, and shell) from palm oil production has increased markedly. For example, in Malaysia, which is the largest palm oil producer in the world, more than 7 million tonnes of EFB, 4.5 million tonnes of fiber, and 1.9 million tonnes of shell are generated as solid wastes, at an increase of 5% annually.[1] Presently, most of the wastes are incinerated or utilized as boiler fuels for steam generation in some palm oil mills.[2] They are also used in part to produce chemicals such as activated carbons and cellulose.[1,3] These processes generally have low efficiency and aggravated environmental problems. Therefore, new technologies with improved efficiencies and reduced environmental impacts to treat this tremendous amount of waste must be established in a timely manner.

Palm oil wastes are high-potential biomass energy sources that are CO_2 neutral. Pyrolysis is considered to be one of the promising thermal approaches in converting biomass to energy.[4−7] However, it is a highly complex process that is influenced not only by the properties of biomass feedstock,[8−16] such as substrate composition, moisture content, and particle size distribution, but also by the operating conditions.[9−16] Fundamentals of biomass pyrolysis have been widely in-

* Author to whom correspondence should be addressed. Telephone: 65-67943244. Fax: 65-67921291. E-mail address: ryan@ntu.edu.sg.
† Nanyang Technological University.
‡ Huazhong University of Science and Technology.

(1) Mae, K.; Hasegawa, I.; Sakai, N.; Miura, K. *Energy Fuels* **2000**, *14*, 1212−1218.
(2) Mahlia, T. M. I.; Abdulmuin, M. Z.; Alamsyah, T. M. I.; Mukhlishien, D. *Renewable Energy* **2003**, *28*, 1235−1256.
(3) Lua, A. C.; Guo, J. *Carbon* **1998**, *36* (11), 1663−1670.
(4) Islam, M. N.; Zailani, R.; Ani, F. N. *Renewable Energy* **1999**, *17*, 73−84.
(5) McKendry, P. *Bioresour. Technol.* **2002**, *83*, 47−54.
(6) Cukierman, A. L.; Rocca, P. A. D.; Bonelli, P. R.; Cassanello, M. C. *Trends Chem. Eng.* **1996**, *3*, 129−144.
(7) Demirbas, A. *Energy Convers. Manage.* **2001**, *42*, 1357−1378.
(8) Blasi, C. D. *Fuel* **1997**, *76* (10), 957−964.
(9) Chen, G.; Andries, J.; Luo, Z.; Spliethoff, H. *Energy Convers. Manage.* **2003**, *44*, 1875−1884.
(10) Beaumount, O.; Schwob, Y. *Ind. Eng. Chem. Process Des.* **1984**, *23*, 637−641.
(11) Blasi, C. D.; Signorelli, G.; Russo, C. D.; Rea, G. *Ind. Eng. Chem. Res.* **1999**, *38*, 2216−2224.
(12) Li, S. G.; Xu, S. P.; Liu, S. Q.; Yang, C.; Lu, Q. H. *Fuel Process. Technol.* **2004**, *85*, 1201−1211.
(13) Lappas, A. A.; Samolada, M. C.; Iatridis, D. K.; Voutetakis, S. S.; Vasalos, I. A. *Fuel* **2002**, *81* (16), 2087−2095.
(14) Encinar, J. M.; Beltran, F. J.; Bernalte, A.; Ramiro, A.; Gonzalez, J. F. *Biomass Bioenergy* **1996**, *11* (5), 397−409.
(15) Raveendran, K.; Ganesh, A.; Khilar, K. C. *Fuel* **1996**, *75* (8), 987−998.
(16) Zhang, J. L. Pyrolysis of Biomass, M.S. Thesis, Mississippi State University, December 1996.

10.1021/ef030193m CCC: $27.50
Published on Web 10/02/2004

vestigated using fluidized-bed reactors,[13] fixed-bed reactors and thermogravimetric analysis (TGA),[12,15] and other reactors.[11,14,16] The use of TGA has the advantage of a fast and repeatable data collection of pyrolysis rate, which facilitates a deep investigation of the kinetic parameters. Previous investigations of biomass pyrolysis were mostly focused on the yields of solid, liquid, and gas products, as a function of the variable parameters, including heating rate, sample size, final temperature, and volatiles residence time.[8−16] However, the real-time gas release in the course of pyrolysis, which is believed to be closely related to the mechanisms of biomass decomposition, is rarely studied. A better understanding of the fundamentals and mechanisms in pyrolysis is essential to achieve high yields of the targeted products.

Cellulose, hemicellulose, and lignin are the main components of lignocellulosic biomass samples. Usually, biomass materials contain 40−60 wt % cellulose, 20−40 wt % hemicellulose, and 10−25 wt % lignin on a dry basis.[17] Previous studies[18−21] have indicated that being able to distinguish the physical and chemical characteristics of the three components is important for a better understanding of biomass pyrolysis. Biomass pyrolysis generally proceeds through a series of complex reaction pathways. At low heating rates (<100 °C/min), biomass materials decompose in well-described stages of moisture evolution, hemicellulose decomposition, and cellulose decomposition.[15,22] Raveendran et al.[15] found that no interaction occurs among the three main biomass components. Some researchers believed that the mechanism of wood pyrolysis is a superposition of the mechanisms of the three components.[15,23] One or all of the three components have been used as model biomass in previous studies.[19−21]

So far, although several studies[8−22] have been reported, the fundamentals relative to the pyrolysis of biomass have not been fully understood. In addition, the pyrolysis of palm oil wastes, which is the representative biomass waste locally, have rarely been studied. This paper determines the characteristics of three palm oil wastes that have been subjected to pyrolysis under different operating conditions in TGA, and the real-time evaluation trends of gas products from pyrolysis are investigated using an integrated system of TGA and Fourier transform infrared (FTIR) spectroscopy. Three components (cellulose, hemicellulose, and lignin) were used as the model biomass in this study, to facilitate the development of a pyrolysis model in the future and also the interpretation of the obtained experimental results. A better understanding of the biomass pyrolysis process is achieved and the fundamentals in the pyrolysis of palm oil wastes is explored for developing an advanced thermal processes for biofuel production from palm oil wastes at improved efficiency and product yields.

Table 1. Particle-Size Distribution of Biomass Samples

	Content (wt %)		
particle size (μm)	shell waste	fiber waste	EFB waste
850−1000	8.71	0.46	0.73
425−850	35.40	1.94	2.44
250−425	17.78	11.78	7.23
150−250	18.37	25.56	14.15
125−150	11.93	33.92	8.69
75−125	6.65	24.26	42.34
<75	1.17	2.07	24.42

2. Materials and Methods

2.1. Materials. The three palm oil wastes—shell, fiber, and empty fruit bunches (EFB)—were obtained from Malaysia. They were ground in a laboratory-scale centrifugal mill (Rocklabs, New Zealand) and sieved in a Retsch test sieve with a 1-mm screen (Retsch, Fisher Scientific Company, USA); i.e., all the samples studied here were <1 mm in size. Their particle size characteristics are listed in Table 1. Compared to the other two samples, shell waste is more difficult to grind, with its particle size mostly in the range of 150−850 μm. EFB and fiber particles are finer, with their particles size mostly <125 μm and in the range of 125−150 μm, respectively.

The proximate analysis of the palm oil wastes was conducted via TGA (TA model 2050, USA). The moisture content was evaluated at 105 °C, the volatiles content was determined at 900 °C under N_2 purging,[24] and the ash content was analyzed at ∼550 °C.[25] The ultimate analysis was performed in a Perkin−Elmer model 2400II CHNS/O analyzer. The results of the proximate and ultimate analyses are shown in Table 2. Palm oil wastes contain a very high volatiles content (>70 wt %) and a low fixed-carbon content (<20 wt %). The low heating value (LHV) of the studied samples (∼20 MJ/kg), measured in a bomb calorimeter (Parr 1260, Parr Instrument Company, Moline, IL), is lower than that of coal, which is possibly due to the low fixed-carbon and high oxygen contents found in the samples.[17] The ultimate analysis indicates that palm oil waste is environmentally friendly, with a trace content of nitrogen and sulfur and mineral matters. If only considering the main elements (C, H, O), the molecular formula of the studied samples, based on one C atom, can be written as CH_xO_y, as listed in the last column of Table 2.

Three components (cellulose, hemicellulose, and lignin) were also analyzed under the same conditions as used for palm oil wastes. Cellulose and lignin were purchased from Sigma−Aldrich Chemie GmbH. The former is in fibrous powder form, and the latter is in the form of a brown alkali powder. Commercial hemicellulose is difficult to obtain, whereas xylan, although it might have different physical and chemical properties, has been widely used as a representative of hemicellulose in pyrolysis processes.[19−21] Here, xylan that was in the form of yellow powders, processed from birchwood and also obtained from Sigma−Aldrich Chemie GmbH, was used as hemicellulose. The average particle size of xylan is ∼100 μm, and those of cellulose and lignin are each ∼50 μm; they are much finer than the three palm oil wastes.

2.2. Equipment and Procedures. The pyrolysis of biomass was conducted in a thermogravimetric analyzer (model TGA 2050, from TA, USA). To choose a reasonable total flow rate of N_2 and sample mass, two pre-experiments were conducted: (i) experiments varying sample mass (2−25 mg) at a fixed N_2 flow rate (40 mL/min), and (ii) experiments varying the N_2 flow rate (40−120 mL/min) at a fixed mass sample (25 mg). The detailed results are not presented here, because of space limitations. Hereafter, a brief description is given. Varying the initial sample mass at the range of 10−25

(17) McKendry, P. *Bioresour. Technol.* **2003**, *83*, 37−46.
(18) Blasi, C. D. *J. Anal. Appl. Pyrolysis* **1998**, *47*, 43−64.
(19) Varhegyi, G.; Antal, M. J. J.; Jakab, E.; Szabo, P. *J. Anal. Appl. Pyrolysis* **1997**, *42*, 73−87.
(20) Orfao, J. J. M.; Antunes, F. J. A.; Figueiredo, J. L. *Fuel* **1999**, *78*, 349−358.
(21) Rao, T. R.; Sharma, A. *Energy* **1998**, *23* (11), 973−978.
(22) Connor, M. A.; Salazar, C. M. In *Research in Thermochemical Biomass Conversion*; Bridgewater, A. V., Knester, J. L., Eds.; Elsevier: London, 1988; pp 164−178.
(23) Stamm, A. J. *Ind. Eng. Chem.* **1956**, *48* (3), 413−417.
(24) Mayoral, M. C.; Izquierdo, M. T.; Andres, J. M.; Rubio, B. *Thermochim. Acta* **2001**, *370*, 91−97.
(25) Mattsson, J. E. Country Report on Standardization of Solid Biofuels in Sweden, No. 22187071, April 2000.

Table 2. Proximate and Ultimate Analyses of Biomass Samples

waste	Proximate Analysis (wt %)[a] moisture, M_{ad}	volatile matter, V_{ad}	ash, A_d	fixed carbon, FC_{ad}	Ultimate Analysis (wt %, db) C	H	N	S	O[b]	low heat value, LHV (MJ/kg)	molecular formula
shell	5.73	73.74	2.21	18.37	53.78	7.20	0.00	0.51	36.30	22.14	$CH_{1.61}O_{0.51}$
fiber	6.56	75.99	5.33	12.39	50.27	7.07	0.42	0.63	36.28	20.64	$CH_{1.69}O_{0.54}$
empty fruit bunches, EFB	8.75	79.67	3.02	8.65	48.79	7.33	0.00	0.68	40.18	18.96	$CH_{1.80}O_{0.62}$

[a] Subscripts represent the following: "ad", air-dried basis; "d", dry basis. [b] The oxygen content was determined by difference.

mg has no significant influence on shell pyrolysis at a flow rate of 40 mL/min, although when sample size was even smaller (2 mg), pyrolysis of the shell waste moved primarily to lower temperatures, which indicates that mass and heat transfer inside the sample particles is negligible with a sample mass that changes from 10 mg to 25 mg. A mass of 25 mg (a large size) was thus chosen in this study to highlight the gas products that are released and the potential influence of sample particle size to be investigated. Moreover, varying the flow rate of N_2 from 40 mL/min to 120 mL/min did not have significant influence on the shell pyrolysis (at a sample mass of 25 mg), indicating that a flow rate of >40 mL/min is large enough to mitigate the potential difference caused by external heat and mass transfer in the gas phase. Purified nitrogen (99.9995%) at a constant flow rate of 40 mL/min was used as the carrier gas to provide an inert atmosphere for pyrolysis and remove the gaseous and condensable products, thus minimizing any secondary vapor-phase interactions. The sample was heated at 10 °C/min, first from ambient to 150 °C and then keeping it at that temperature for 10 min to remove moisture. It was then heated to 900 °C and kept at that temperature for 3 min. In the following text, unless otherwise noted, the experimental conditions remained the same.

2.3. Calculation of Kinetic Parameters. A kinetic study of biomass pyrolysis is necessary to achieve an efficient production of fuel gases, chemicals, and energy. The information gained is also of utmost importance for the proper design of large-scale pyrolysis reactors.[18−21] Under the selected conditions of sample mass (25 mg) and total flow rate (40 mL/min) in this study, the gas-phase and internal mass- and heat-transfer limitation could be negligible. The biomass pyrolysis is assumed to be controlled primarily by chemical decomposition, and the kinetic parameters (activation energy and reaction order) could be calculated, based on the following principles.

Assuming a general thermal decomposition equation, such as eq 1, which could occur in the biomass pyrolysis in TGA,

$$\mathrm{A}(s) \rightarrow \mathrm{B}(s) + \mathrm{C}(g) \tag{1}$$

the dynamics of the reaction can be symbolized as eq 2.

$$\frac{\mathrm{d}\alpha}{\mathrm{d}t} = kf(\alpha) \tag{2}$$

Here, A(s) represents the reactant−solid biomass, B(s) represents solid residue from the biomass pyrolysis at high temperature, and C(g) represents the gas products. According to the Arrhenius equation, $k = A\ \exp[-E/(RT)]$, eq 2 can be rewritten as

$$\frac{\mathrm{d}\alpha}{\mathrm{d}t} = A\ \exp\left(-\frac{E}{RT}\right)f(\alpha) \tag{3}$$

where α is the thermal conversion and is given as $\alpha = (W_0 - W)/(W_0 - W_\infty)$, where W is the mass of solid sample and the subscripts "0" and "∞" refer to the initial and final residual amounts, respectively. The term $f(\alpha)$ is the reaction mechanism, and the kinetics parameters E and A represent the activation energy and the pre-exponential factor, respectively; R is the universal gas constant.

Suppose the pyrolysis, as a simple reaction—the dynamics mechanism—can be symbolized as $f(\alpha) = (1 - \alpha)^n$, and n is the reaction order; eq 3 then can be rewritten as

$$\frac{\mathrm{d}\alpha}{\mathrm{d}t} = \left(\frac{1}{\beta}\right)A\ \exp\left(-\frac{E}{RT}\right)(1 - \alpha)^n \tag{4}$$

where β is the heating rate, given as $\beta = \mathrm{d}T/\mathrm{d}t$.

To obtain the kinetics parameters E and A, several methods are available.[26] According to our experimental conditions, the nonisothermal method (i.e., the sample was heating at a selected heating rate) was used:[27]

$$G(\alpha) = \int_{T_0}^{T}\left(\frac{A}{\beta}\right)\exp\left(-\frac{E}{RT}\right)\mathrm{d}T \approx \int_{0}^{T}\left(\frac{A}{\beta}\right)\exp\left(-\frac{E}{RT}\right)\mathrm{d}T \tag{5}$$

Usually, for most temperatures and activation energies, $RT/E \ll 1$, and $1 - 2RT/E \approx 1$, so the kinetic mechanism equation can be simplified as

$$\ln[G(\alpha)] = -\left(\frac{E}{RT}\right) + \ln\left(\frac{AR}{\beta E}\right) \tag{6}$$

$$G(\alpha) = -\frac{\ln(1 - \alpha)}{T^2} \qquad (\text{for } n = 1) \tag{7}$$

$$G(\alpha) = \frac{1 - (1 - \alpha)^{1-n}}{(1 - n)T^2} \qquad (\text{for } n \neq 1) \tag{8}$$

If the reaction order is correct, the plot of $\ln[G(\alpha)]$ versus $-1/T$ should be a straight line, the activation energy E can be obtained from the slope, and the pre-exponential factor A can be obtained from the intercept.

Nevertheless, with the change of pyrolysis temperature, the related mechanism might be different, and, as such, the kinetic parameters under different temperatures should be analyzed separately.[18−21] The correct mechanism is ascertained on the basis of best-fit criteria between the experimental and calculated results. When the entire pyrolysis process is divided into several stages, E is just the activation energy of each individual temperature range, which has no direct relation to the entire process. To obtain the overall pyrolysis characteristics, Cumming[28] determined the weight mean activation energy (E_m) and used it to analyze the overall sample reactivity:

$$E_m = (F_1 \times E_1) + (F_2 \times E_2) + \ldots + (F_n \times E_n) \tag{9}$$

where E_1 through E_n is the activation energy of every stage (1 through n), F_1 through F_n is the corresponding relative weight loss amount. Both E for a specific temperature stage and the mean activation energy (E_m) for an overall evaluation of biomass pyrolysis were calculated in this work.

2.4. Fourier Transform Infrared Analysis of Gas Products. Although the kinetic analysis using TGA supplies important information in regard to the pyrolysis of palm oil wastes, including the rate of pyrolysis, temperature range for degradation, reaction order, activation energy, etc., the un-

(26) Galwey, A. K. *Thermochim. Acta* **2004**, *413* (1−2), 139−183.
(27) Chen, J. H.; Li, C. R. *Thermal Analysis and Application* (in Chin.); Science Press: Beijing, 1985.
(28) Cumming, J. W. *Fuel* **1984**, *63* (10), 1436−1440.

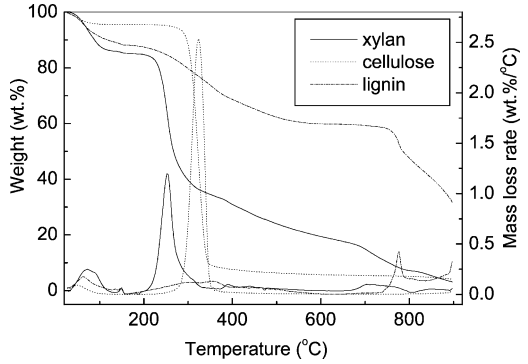

Figure 1. Comparison of pyrolysis of xylan, cellulose, and lignin.

derstanding of the gas species evolved during biomass pyrolysis is still limited. The gaseous products from the pyrolysis of palm oil wastes were investigated using TGA−FTIR. Previous publications have shown that FTIR has been used to analyze the gaseous products from pyrolysis either qualitatively or quantitatively.[29−31]

While other conditions were kept the same as those used in TGA, the flow rate of carrier gas was set at 120 mL/min for FTIR analysis. To minimize the secondary reaction, the gas products released from the biomass pyrolysis in TGA were swept immediately to a cold gas cell, followed by analysis using FTIR equipped with a deuterated triglycine sulfate (DTGS) detector (BioRad Excalibur Series, model FTS 3000). The transfer line and gas cell were heated to an internal temperature of 230 °C, to avoid any condensation or adsorption of semivolatile products. Each IR spectrum was obtained for a time interval of 60 s, and the scanning range was 4000−500 cm^{-1}, in terms of wavenumber. The resolution and sensitivity were set at 2.5 and 1, respectively. The distribution of gaseous products from pyrolysis was analyzed, with respect to the changing of reaction temperatures, from 150 to 900 °C.

3. Results and Discussion

3.1. Biomass Pyrolysis in Thermogravimetric Analysis. The pyrolysis characteristics—both the thermogravimetry curves (TG, in units of wt %) and differential thermogravimetry curves (DTG, in units of %/°C)—of the three components (xylan, cellulose, and lignin) are shown in Figure 1. There are obvious differences between their behaviors. Most of the weight loss due to xylan (the typical hemicellulose) happens from 220 °C to 300 °C. When the temperature is >300 °C, its weight-loss rate (in units of wt %/°C) decreases sharply to zero. The pyrolysis of cellulose focuses at 300−340 °C. In comparison to the sharper DTG peaks of cellulose and hemicelluloses, lignin results in wide and flat DTG peaks. From the ambient temperature to 700 °C, only ∼40 wt % of the lignin weight is lost at a very low rate (<0.15 wt %/°C). It might be attributed to the slow carbonization of lignin, and carbon could be the main product; lignin is the main component responsible for the production of char.[20] Only when the temperature is >750 °C do its weight-loss rates increase slightly (to 0.3 wt %/°C), and a total weight loss of ∼67 wt % is achieved at 850 °C.

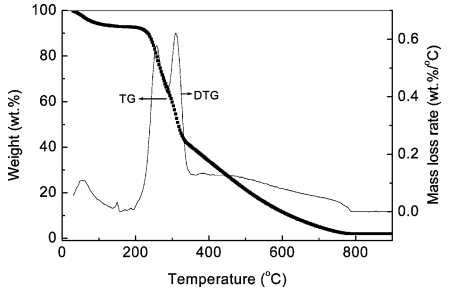

Figure 2. Pyrolysis curves of shell waste.

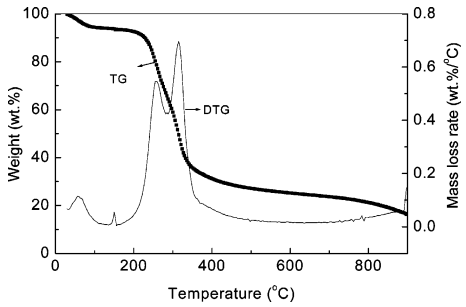

Figure 3. Pyrolysis curves of fiber waste.

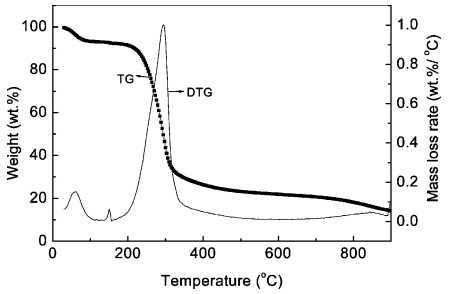

Figure 4. Pyrolysis curves of EFB waste.

The difference of inherent structures and compositions among the three components possibly accounts for the different behaviors observed.[16−19] The cellulose molecule ($[C_6(H_2O)_5]_n$) is a very long polymer of glucose units without any branches, and it is crystalline, strong, and resistant to hydrolysis. In contrast, hemicellulose ($[C_5(H_2O)_4]_n$) has a random, amorphous structure with little strength. It is easily hydrolyzed by a dilute acid or base. Lignin ($[C_{10}H_{12}O_3]_n$) might be established by cross-linking; the large lignin molecules fill three dimensions and are heavily cross-linked. In terms of thermal degradation, the three components, in order from the easiest to the most difficult, are as follows: hemicellulose > cellulose > lignin.[7]

The pyrolysis curves of the three palm oil wastes are plotted in Figures 2(shell waste), 3 (fiber waste), and 4 (EFB waste). They start to degrade at ∼220 °C and the weight loss starts promptly after that temperature. When the temperature is >340 °C, no obvious weight loss is observed. Moisture is generally removed at 105 °C. The main differences between the three samples are observed in their DTG curves: the shell and fiber wastes have two peaks, but the EFB waste has just one. It is possibly related to the different volatiles and fixed-carbon contents that exist in the wastes (see Table 2). EFB waste had a much higher volatiles content and lower fixed-carbon content, compared to the other two wastes. The release of volatiles potentially causes an

(29) Bassilakis, R.; Carangelo, R. M.; Wojtowicz, M. A. TG-FTIR Analysis of Biomass Pyrolysis. *Fuel* **2001**, *80*, 1765−1786.
(30) Wojtowica, M. A.; Bassilakis, R.; Smith, W. W.; Chen, Y. G.; Carangelo, R. M. *J. Anal. Appl. Pyrolysis* **2003**, *66*, 235−261.
(31) Saade, R. G.; Kozinski, J. A. *Biomass Bioenergy* **2000**, *18*, 391−404.

Table 3. Kinetics Parameters of the Biomass Samples

temp range (°C)	n	activation energy, E (kJ/mol)	A (s^{-1})	correlation coefficient, R	weight loss (wt %)	E_m (kJ/mol)
			Xylan Biomass			
220−300	1	69.39	2.0921×10^3	0.9902	44.0	69.39
			Cellulose Biomass			
300−340	1	227.02	5.6×10^{16}	0.9993	75.0	227.02
			Lignin Biomass			
220−380	1	7.80	4.91×10^{-5}	0.9926	16.44	33.22
380−530	3	8.20	1×10^{-4}	0.9973	9.14	
750−900	1	54.77	3.4×10^{-2}	0.9907	30	
			Shell Biomass			
220−300	1	55.64	2.82×10^1	0.9936	32.0	62.85
300−340	1	75.72	2.4276×10^3	0.9991	17.9	
			Fiber Biomass			
220−300	1	51.82	1.03×10^1	0.9967	32.3	58.64
300−340	1	67.68	3.644×10^2	0.9980	24.4	
			EFB Biomass			
220−300	1	59.50	7.74×10^1	0.9868	46.1	61.35
300−340	1	67.58	6.197×10^2	0.9953	13.6	

earlier degradation of carbon, resulting in one big peak. However, shell and fiber wastes contained a much higher fixed-carbon content and, thus, were more difficult to degrade. Their two separated peaks represent, respectively, the release of volatiles and the degradation of carbon.

The three components (cellulose, hemicellulose, and lignin) had individually significant roles in determining the pyrolysis characteristics of the biomass, which is specific for each type of biomass under a given operating condition. As for the studied palm oil wastes, although there were some differences, in terms of the onset and end temperatures of pyrolysis, their degradation can also be separated into several stages, as follows:

Zone I (<220 °C): In this region, moisture evolution occurs. In fact, at ∼100 °C, all the moisture has been removed. In the temperature range of 100−220 °C, no obvious weight loss is observed (see Figures 2−4).

Zone II (220−300 °C): In this region, predominantly hemicellulose (xylan) decomposition occurs (see solid curves in Figure 1).

Zone III (300−340 °C): In this region, mainly cellulose decomposition occurs (see dotted curves in Figure 1).

Zone IV (>340 °C): In this region, mainly lignin decomposition occurs (see dashed curves in Figure 1).

3.2. Kinetic Calculation Results. The weight loss of the studied palm oil wastes occurred mainly at 220−340 °C; thus, this temperature range was considered for the calculation of kinetic parameters, i.e., only the decompositions of hemicellulose (Zone II, 220−300 °C) and cellulose (Zone III, 300−340 °C) were calculated.

To determine the kinetic parameters, different reaction orders (n = 0, 0.5, 1, 2, and 3) were assumed and the kinetic parameters were calculated using eqs 6−9. The reaction order is ascertained based on best-fit criteria. Table 3 shows that n = 1 is the best fit for the pyrolysis of palm oil wastes and the three components of biomass (except for lignin at 380−530 °C), where the correlation coefficients (R) are all >0.99. It can be observed that the E_m values of the three components are different, whereas those of palm oil wastes are quite similar. Compared to xylan and cellulose, lignin has an extremely low activation energy (∼33 kJ/mol) and its corresponding pre-exponential factor is also very low. Similar observations were previously reported by Varhegyi et al.[19] The much lower activation energy of xylan than cellulose is probably caused by the differences in their structures.[16−19] Previous publications indicate that the activation energy (E) of cellulose in pyrolysis is generally ∼200 kJ/mol; for hemicellulose, it is relatively low, at ∼100 kJ/mol; and for lignin, it is much lower, only ∼30 kJ/mol.[19−21] The activation energy of the biomass in pyrolysis is ∼70−100 kJ/mol.[20] Our results are consistent with those of other researchers. The different activation energies between palm oil wastes and the three components (particularly cellulose) may be caused by the catalytic effect of mineral matters that occur in the biomass.[19,32,33] Moreover, for the three palm oil wastes, the E values of the second range (300−340 °C), referring to the degradation of cellulose, are always larger than those of the first range (220−300 °C), which refers to the degradation of hemicellulose. This difference is possibly caused by their different structures, as discussed previously.[16−19] However, further studies are needed to understand this issue better.

3.3. Influence of Operating Parameters on Biomass Pyrolysis. *3.3.1. Influence of Heating Rate.* The heating rates in this study were varied as follows: 0.1, 0.5, 1, 5, 10, 20, 35, 50, 80, and 100 °C/min. The representative DTG curves of cellulose, relative to the change of heating rate, are plotted in Figure 5. The initial reaction temperature (T_i), the temperature at the maximum mass loss rate (T_{max}), the peak value of mass loss rate, and the final temperature (T_f) of cellulose pyrolysis under different heating rates are listed in Table 4 (only those at heating rates up to 20 °C/min

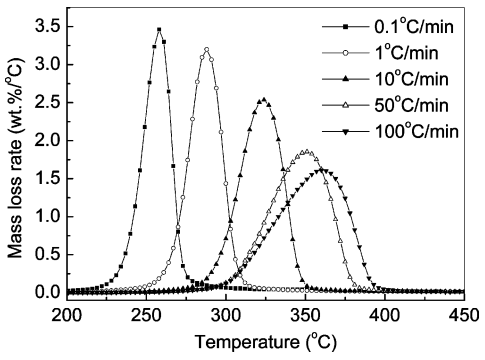

Figure 5. Pyrolysis of cellulose under different heating rates.

Table 4. Cellulose Pyrolysis in Thermogravimetric Analysis at Different Heating Rates

heating rate (°C/min)	T_i (°C)	T_{max} (°C)	peak value (wt %/°C)	T_f(°C)	E (kJ/mol)	A (s^{-1})	correlation coefficient, R
0.1	230	257	3.59	280	203.50	9.0×10^{14}	0.9898
0.5	250	280	3.38	300	216.58	1.4×10^{16}	0.9917
1	260	290	3.26	310	232.75	3.6×10^{17}	0.9962
5	280	310	3.01	330	217.32	9.0×10^{15}	0.9959
10	290	325	2.54	350	207.68	9.8×10^{13}	0.9969
20	295	334	2.74	350	206.36	1.1×10^{15}	0.9891

are given). Figure 5 shows that the T_i and T_f values increase as the heating rate increases, and the peaks of the DTG curves widen and smoothen. At a very low rate (0.1 °C/min), the pyrolysis begins at 230 °C and ends at 280 °C. When the rate is increased to 100 °C/min, the reaction begins at 310 °C with an end at ~400 °C. The temperature of the maximum mass loss rate is delayed, and its maximum value also decreased largely. The kinetic parameters of cellulose under different heating rates were also calculated, using the integration method (eq 6). According to our previous results (see Table 3) and the literature,[18−20] the reaction order for cellulose was preset at 1 (see Table 4). The correlation coefficients under different heating rates were $R \approx 0.99$, indicating that the assumed reaction order ($n = 1$) was fit for cellulose pyrolysis. Table 4 shows that the activation energies are quite similar to each other (~200 kJ/mol) as the heating rate is varied from 0.1 °C/min to 20 °C/min. However, a slight decrease in activation energy was observed with a further increase of the heating rate to >35 °C/min, finally reaching an activation of ~150 kJ/mol at a heating rate of 100 °C/min. At the same time, an obvious decrease of the pre-exponential factor A was also observed at heating rates of >35 °C/min.

Two peaks were found in the DTG curves of shell pyrolysis, and as the heating rate increases, the two peak temperatures moved to higher values (not shown here). The beahvior of fiber waste is similar to that of shell waste; as the heating rate increased, the first peak of the fiber waste moved to a higher temperature and its peak value became larger, and at the same time, its weight loss occurred over a wider temperature range. The DTG curves of EFB waste under different heating rates were also obtained, and the results are quite similar to those found with cellulose.

The changes in the characteristic temperatures (T_i, T_{max}, T_f) related to biomass pyrolysis at different heating rates are most likely associated with the differences of heat and mass transfer of the sample particles internally or externally. At lower heating rates, samples are heated uniformly from the inside to the outside, the sample decomposes promptly, and the mass is lost quickly. The maximum value of mass loss rate is also enhanced (see Figure 5). In contrast, at higher heating rates, there is a large thermal gradient within the sample particles. With further increases in the heating rate, the temperature difference inside a sample particle is also enlarged. Although the characteristic temperatures changed largely with the heating rate, increasing from 0.1 °C/min to 20 °C/min, the calculated activation energies are constant (~200 kJ/mol), indicating that the heat-transfer limits are not significant for these cases. Our previous results of kinetic parameters shown in Table 3 at a heating rate of 10 °C/min should be valid. However, at high heating rates (>35 °C/min in this study), the heat-transfer limitation caused by the large thermal gradient within the sample particles becomes more important and the kinetic parameters obtained at a heating rate of >35 °C/min are much lower than its true value, and are most likely invalid, because a purely kinetically controlled regime is assumed to calculate those kinetic parameters. This observation of decreased activated energy at high heating rates is consistent with Blasi's result.[18]

3.3.2. Influence of Particle Size. The pyrolysis curves of shell waste at different particle sizes are plotted in Figure 6. Particle-size changes over a wide range (from 250 μm to >2 mm) do not have significant influence on the shell pyrolysis, which indicates the minor influence of internal heat/mass transfer on pyrolysis, similar to the previous report.[14] The rate of pyrolysis became faster with the further decrease of particle size to <75 μm; the two peaks become closer and even are overlapped. This might be due to the heat- and mass-transfer differences that exist between the internal and external particles. For a larger particle, a longer time is required to heat it and release the volatile matters. The kinetic parameters of shell samples under different particle sizes were also calculated (eqs 6−9), and the results are listed in Table 5 (except for sample sizes of <75 μm). The activation energies of the second temperature range are always larger than those of the first range. The activation energies (E_m) for the particles ranging in size from 250 μm to >2 mm are quite similar (~65 kJ/mol), whereas for those <75 μm in size, the activation energy increased to 70 kJ/mol (not shown in Table 5), implying a regime probably controlled by not only kinetics but also mass/heat transfer. In the latter case (particle sizes of <75 μm), the calculated kinetic parameters might be invalid. The samples used to obtain kinetic parameters (see Table 3) were original and not distinguished in particle size. With a small portion (1−2 wt %) of particles <75 μm in size (see Table

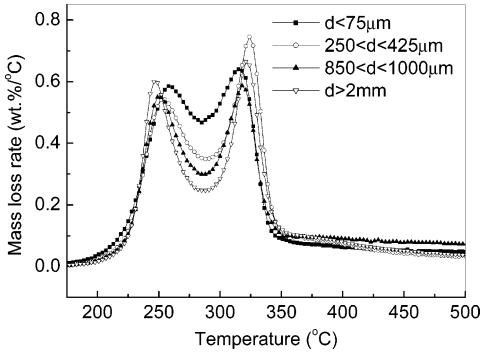

Figure 6. Pyrolysis of shell waste with different particle sizes.

(32) Blasi, C. D. *Thermochim. Acta* **2000**, *364*, 133−142.
(33) Williams, P. T.; Horne, P. A. *Renewable Energy* **1994**, *4* (1), 1−13.

Table 5. Kinetic Parameters of Shell Waste Samples with Different Particle Sizes

temp (°C)	E (kJ/mol)	A (s^{-1})	correlation coefficient, R	mass loss (wt %)	E_m (kJ/mol)
		Particle Size = 250−425 μm			
220−300	48.06	4.8×10^0	0.9924	29.5	66.31
300−340	91.33	6.5×10^4	0.9665	21.6	
		Particle Size = 850−1000 μm			
220−300	47.68	5.0×10^0	0.9897	27.8	65.05
300−340	93.39	1.2×10^5	0.9826	17.1	
		Particle Size = >2000 μm			
220−300	46.00	3.3×10^0	0.9806	26.3	64.55
300−340	91.04	6.3×10^4	0.9674	18.4	

1), the kinetic parameters calculated for shell and fiber wastes should be valid; however, those for EFB waste are uncertain, because ~25 wt % of the EFB particles are <75 μm in size. A further investigation of EFB waste with consideration of the different particle sizes to calculate kinetic parameters is needed.

3.4. Thermogravimetry-Fourier Transform Infrared Analysis of Gas Products. Generally, the following gas species evolve during the pyrolysis of most organics and biomass: CH_4, C_2H_4, CO_2, CO, H_2O, NH_3, HCN, SO_2, and COS. The distribution of these gas products is dependent on the associated elements that are present in the sample.[29] A typical spectral output from the TGA−FTIR of fiber pyrolysis is shown in Figure 7; it is known as a stack plot. The IR spectra taken every minute in the experiment are plotted one on top of the other; a total of 75 IR scans formed the three-dimensional spectra, which indicated the evolution of gas products during the course of pyrolysis of the fiber waste, as a function of both wavenumber and time or temperature. As can be observed from Figure 7, the main gas products of palm oil wastes are CO_2, H_2O, CH_4, CO, and some organics. The gas products begin to evolve at ~230 °C, and most gas species evolve out at 260−350 °C; this corresponds with the previous results obtained from the thermoanalysis. The release of CO_2 and CH_4 first increases as the temperature increases and reaches their maximum yields at ~330 and 340 °C, respectively. However, as the temperature increases further, the evolution of methane is decreased sharply after its peak point and remains low until a temperature of 900 °C is reached. In regard to CO_2, there is also a sharp decrease in its evolution until a temperature of 400 °C is attained. Beyond that temperature, it starts to increase slightly. CO has demonstrated performance similar to that of CO_2, except its maximum evolution occurs at ~270 °C. Among the gas species, only CO_2 is evolved when the temperature is >350 °C. For the other two samples (EFB and shell wastes), similar results are observed, except that their CH_4 evolution is very small; almost no CH_4 yield is observed with FTIR for the EFB and shell wastes.

In the gaseous products, there are also a few organics (C_2 acids, ether, and other hydrocarbon compounds). However, their concentrations are often too low to be detected.[34] In addition, those gases (such as H_2, N_2, O_2, and H_2S) have no or weak IR absorption; thus, they are impossible to detect using FTIR.[29] However, this approach provides a rapid FTIR scan within seconds, which facilitates our research on the kinetics and gaseous species evolution. Determination of the evolution rate and modeling of the gas-product release process under various operating conditions will be studied in detail in our future study.

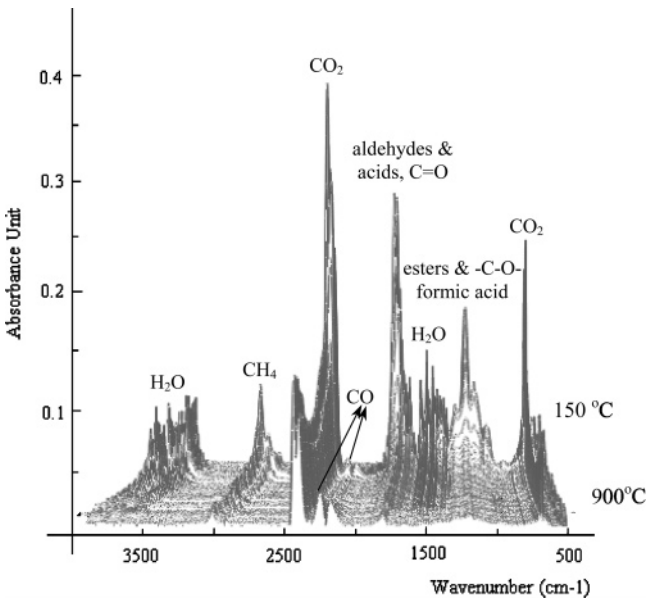

Figure 7. Infrared (IR) stack plot from the pyrolysis of fiber waste in thermogravimetry−Fourier transform infrared (TGA−FTIR) spectroscopy.

4. Conclusions

Palm oil wastes are the major agriculture wastes in countries in southeast Asia. In this study, their thermoanalysis, under different operating conditions, were performed to obtain a basic understanding of the pyrolysis of palm oil wastes. At the same time, the pyrolysis gaseous products were identified using Fourier transform infrared (FTIR) spectroscopy. The conclusions that can be reached are as follows:

(1) Palm oil wastes contain ~50 wt % carbon, 7 wt % hydrogen, and a trace amount of ash. They have a volatiles content of 70 wt %, a low heat value (LHV) of 20 MJ/kg, and almost no nitrogen and sulfur. They are ideal waste sources for clean energy production.

(2) Thermogravimetric analysis (TGA) showed that palm oil wastes are easily degraded. Their pyrolysis processes can be divided into four stages, by virtue of their specific characteristics and through a comparison with the pyrolysis properties of the three components (hemicellulose, cellulose, and lignin). The four stages are moisture evolution (<220 °C), hemicellulose decomposition (220−300 °C), cellulose decomposition (300−340

(34) Ulmgren, P.; Radestrom, R.; Edblad, M.; Wennerstrom, M. *J. Pulp Paper Sci.* **1999**, *25*, 344−350.

°C), and lignin decomposition (>340 °C). The weight loss of the studied palm oil wastes is focused in the temperature range of 220−340 °C. The activation energy is only ~60 kJ/mol, and the degradation of palm oil wastes is generally a first-order reaction under the studied conditions: sample mass (10−25 mg), flow rate (40−120 mL/min), heating rate (0.1−20 °C/min), and particle size (>75 μm).

(3) With increasing heating rates, the pyrolysis of palm oil wastes occurred at a higher temperature and the mass loss rate decreased, and the activation energy is kept constant as the heating rate increased from 0.1 °C/min to 20 °C/min. Changing the particle size in the range of 250 μm to >2 mm has no significant influence on pyrolysis.

(4) Gaseous products, as identified by FTIR, are primarily CO_2, CO, CH_4, H_2O, and a few organics. Most gaseous products evolved at 250−350 °C, which is consistent with the observation obtained from the thermoanalysis.

Acknowledgment. H.Y. is very grateful for the collaboration program between the Institute of Environmental Science and Engineering, Nanyang Technological University, Singapore and National Laboratory of Coal Combustion, Huazhong University of Science and Technology, China, which provided her the opportunity to pursue her Ph.D. degree in Singapore under a research scholarship.

EF030193M